Mechanical and Thermal Characterization of Graphene and TiO$_2$-Reinforced 4032 Aluminum Alloy for Piston Applications Using Mean Field Homogenization

Sachin Sigdel[1], Prajjwal Dalal[1], Sagar Sanchaniya[1], Nikunj Rachchh[1], Dhaiwat Trivedi[1*]

[1] Department of Mechanical Engineering, Faculty of Mechanical Engineering, Marwadi University, Rajkot-Morbi Road, At & PO: Gauridad, 360003 Rajkot, Gujarat, India
* Corresponding author, e-mail: dhaiwat.trivedi@marwadieducation.edu.in

Abstract

The impact of adding graphene and titanium dioxide (TiO$_2$) nanoparticles to a 4032 aluminum alloy for use in piston applications is examined in this paper. Mori-Tanaka micromechanical modelling and mean-field homogenization were used to examine the characteristics of the composites. Mechanically, the findings demonstrated that the graphene-reinforced composite outperformed the TiO$_2$-reinforced composite and the base material without reinforcement in terms of tensile strength, elastic modulus. The TiO$_2$-reinforced composite, however, had a higher Poisson's ratio, suggesting that lateral deformation was more likely when crushed axially. The graphene-reinforced composite also had less overall deformation and density than the TiO$_2$-reinforced composite and showed a lower Poisson's ratio. Thermally, the graphene-reinforced composite exhibited higher thermal conductivity, which was particularly significant for piston cooling, and showed overall higher performance characteristics for piston applications. This study sheds light on the use of Mori-Tanaka modelling and mean-field homogenization to forecast the mechanical and thermal characteristics of metal matrix composites.

Keywords

metal matrix, reinforcement, mean field homogenization, Mori-Tanaka

1 Introduction

In the current situation, the demand of aluminum metal is high in many engineering applications such as aerospace industry, biomedical sector, automobile sector etc. Aluminum alloys are preferred in the production of machine parts due to their superior properties to cast iron, which include low density, excellent thermal conductivity [1], high strength at elevated temperature [2], a high strength-to-weight ratio [3], a modest thermal expansion coefficient [1], and excellent resistance to corrosion [4]. The most often utilized piston material is 4032 aluminum [5]. In addition, it is employed in the automotive sector and industry for a variety of engine parts, including pistons, gearbox valves, master brake cylinders, hydraulic applications and many more [6].

Magibalan et al. [7] have discussed the use of Metal-Matrix Composites (MMCs) in engineering applications, particularly in the aerospace industry. MMCs are engineered combinations of two or more materials, one of which is a metal, that achieve tailored properties through the systematic combinations of different constituents. The limitations of conventional monolithic materials in achieving high combinations of strength, stiffness, and density make MMCs a popular choice in many industrial applications where specific strength, weight, and cost are important factors.

Rao and Padmanabhan [8] examined the fabrication of aluminum alloy-boron carbide composites through liquid metallurgy techniques with different particulate weight fractions. They found that the density of the composites decreased as the amount of boron carbide increased, while the hardness and compressive strength increased. Ravichandran et al. [9] synthesized and studied the forming behavior of aluminum-based hybrid powder metallurgic composites, while Balasivanandha Prabu and Karunamoorthy [10], through a 2-dimensional microstructure-based finite element analysis (FEA) model that took particle clustering effects into account, analyzed the mechanical behavior of MMC. Sozhamannan et al. [11] used a methodology of microstructure-based elastic-plastic

FEA to predict the failure of two-dimensional microstructure models of Particle Reinforced Metal Matrix Composites (PRMMC). They analyzed the effects of random and clustered particles on the strength and failure mechanisms. In our case we have considered 4032 aluminum as the matrix material and the analysis has been conducted based on its properties.

Tiwari et al. [12] explained the unique qualities of graphene, a 2D substance, which make it extremely beneficial for a variety of applications. Because of its exceptional electrical conductivity and distinctive electronic characteristics, graphene is ideally suited for next-generation technology. Graphene also has outstanding heat conductivity; however, it is substrate dependent. Additionally, graphene possesses superb mechanical qualities. The half-integer Quantum Hall Effect in graphene is likewise unusual and demonstrates a remarkable correlation between charge, thickness, and the speed of the charge carriers. Graphene is the ideal material for many contemporary technologies since it possesses a number of amazing qualities that are not seen in other non-metallic materials. Along with several other materials as substrate or template, graphene serves as the ideal material for many contemporary technological applications. Graphene is known to be the strongest material ever tested, with a tensile strength of over 130 GPa, which is more than 100 times stronger than steel [13]. This property is due to the strong covalent bonds between carbon atoms in the graphene lattice. Graphene is also very stiff, with a Young's modulus of 1 TPa, which is the highest reported for any material. This means that even small deformations in graphene require a significant amount of force.

Kashinath et al. [14] have discussed the synthesis and properties of graphene and graphene oxide, including their potential applications in electrochemical, energy storage, cell imaging, drug delivery, and biosensors. It covers their characterization by XRD, Raman, FT-IR, UV, and SEM, and the different peaks observed in XRD studies. The modified Hummer's method is used to synthesize graphene oxide from natural graphite powder, while graphene is synthesized by reducing graphene oxide using hydrazine hydrate. The main objective of using graphene was to improve thermal conductivity of composite so that it will impact on the heat transfer rate, and it would lead to increase the strength to weight ratio.

Dahl et al. [15] discusses titanium dioxide (TiO_2) composite nanomaterials, covering their manufacture and various domains of use. For the purpose of developing composites, TiO_2 needs to be combined with a variety of other materials. This could be done in a variety of approaches. According to particular metals, material kinds, nanocide semiconductors, carbon, and templated composites, the review classifies composites. Additionally mentioned are the benefits of TiO_2 composites. Due to its exceptional qualities, including a high refractive index, great chemical stability, and good photocatalytic activity, titanium dioxide (TiO_2) is a material that is often utilized in a variety of applications. TiO_2's high opacity and brightness make it a popular pigment in paints, coatings, and polymers. TiO_2 is also used to make solar cells, as a catalyst in a number of chemical processes, and as an ingredient in cosmetics and culinary items [16]. Having a crystalline structure with tetragonal symmetry, TiO_2 is a ceramic substance. It is a white, odorless powder that is soluble in a few organic solvents, including water. TiO_2 is very dense and has a high melting point (1843 °C).

The mechanical and thermal behavior of 4032 aluminum composites enhanced with graphene and TiO_2 is examined in this work. Finite Element Analysis (FEA), mean-field homogenization, and Mori-Tanaka modeling are used to assess important characteristics like deformation, Poisson's ratio, Young's modulus, and thermal conductivity. The results will help with piston material optimization for high-temperature and high-load scenarios.

Table 1 shows the composition of 4032 aluminum. Overheating of the piston leads to premature wear of the friction surfaces, sticking and failure of the piston rings, seizure of the piston, burning of the piston crown, etc. [17]. The study included a pre-designed piston model for an existing commercial passenger automobile, with petrol as its operating fuel. The approach is to conduct finite element analysis for finding out thermal conductivity and mechanical properties of each composite material fabricated with 10 specific combinations of reinforcement materials, varying by their weight percentage as shown in Table 1.

2 Mean field homogenization

Homogenization techniques are the methods that are used to calculate the effective properties of a composite material by analyzing the microstructure of the material. These techniques are often based on direct finite element analysis of Representative Volume Elements (RVE) at the micro scale using macroscopic values as the boundary conditions. The computed results are then returned to the macro scale by averaging techniques. This approach is highly accurate and provides detailed micro fields. Mean

Table 1 Homogenized properties of aluminum matrix using TiO$_2$ and graphene reinforcement, M0† is 4032 Al alloy without added reinforcements

| Material	Reinforcement material	Reinforcement weight %	Young's modulus (Pa)	Poisson's ratio	Density (kg/m³)	Thermal conductivity (W/m K)
M0†	-	-	7×10^{10}	0.33	2690	155
M1	Graphene	0.5%	7.0637×10^{10}	0.32952	2687.9	157.13
M2	Graphene	1%	7.1297×10^{10}	0.32904	2685.8	159.28
M3	Graphene	1.5%	7.1927×10^{10}	0.32857	2683.7	161.45
M4	Graphene	2%	7.258×10^{10}	0.32809	2681.6	163.64
M5	Graphene	2.5%	7.3239×10^{10}	0.32762	2679.5	165.85
M6	TiO$_2$	0.5%	7.0384×10^{10}	0.32969	2696.6	153.89
M7	TiO$_2$	1%	7.077×10^{10}	0.32939	2703.1	152.79
M8	TiO$_2$	1.5%	7.1157×10^{10}	0.32909	2709.6	151.7
M9	TiO$_2$	2%	7.1547×10^{10}	0.32878	2716.2	150.6
M10	TiO$_2$	2.5%	7.1939×10^{10}	0.32848	2722.8	149.52

field homogenization is a method used to compute thermal and mechanical properties of composite materials. It is a semi-analytical homogenization approach that can be used to predict the influence of microstructure on overall properties. In multi-phase thermo-elastic composites, Eshelby based mean-field homogenization models provide a cost-effective way of predicting the influence of microstructure on overall properties [18]. Sharma et al. [19] have discussed how mean-field homogenization can be used to compute thermal and mechanical properties of composite materials and how it can be used to study various types of composite materials, including fiber-reinforced composites, particulate composites, and laminated composites. The Mori-Tanaka method (Fig. 1), a micromechanical model based on Eshelby's equivalent inclusion method, predicts the effective elastic properties of composite materials

by considering two phases (matrix and inclusion) and calculating the average stress and strain in each phase [20].

This model was proposed by Mori and Tanaka [21]. The derivation is based on a rough application of Eshelby's answer. It is discovered that the strain concentration tensor, which relates the volume average of strain across all inclusions to the mean matrix strain, is shown as

$$B^\varepsilon = H^\varepsilon \left(I, C_0, C_1 \right). \tag{1}$$

Nemat-Nasser and Hori [22] suggested the double inclusion (D-I) model. These principles form its foundation. A reference medium of stiffness C_r exists outside of each inclusion (I) of stiffness C_1, whereas the genuine matrix material of stiffness C_0 surrounds each inclusion (I) in its immediate surroundings. To put it another way, the actual composite RVE is changed out for a model composite comprised of a fictional
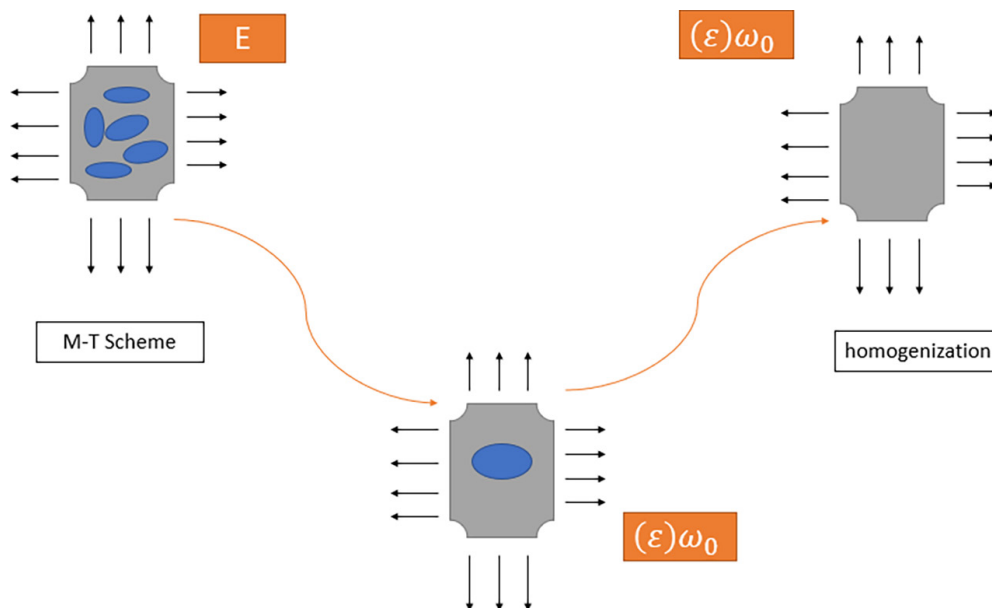
Fig. 1 Illustration of Mori-Tanaka model

reference matrix of stiffness C_r with embedded stiffness C_1 inclusions covered in stiffness C_0 material.

Since several schemes may be created depending on the precise choice of the stiffness of the reference medium, the D-I model is actually a family of MFH models. The demonstration may be made in particular using the following three cases:

- $C_r = \underset{\sim}{C}$ (composite): self-consistent model;
- $C_r = C_0$ (matrix): Mori-Tanaka model;
  $$B^\varepsilon = H^\varepsilon (I, C_0, C_1) \equiv B_l^\varepsilon$$
- $C_r = C_1$ (inclusion): inverse Mori-Tanaka model;
 $$B^\varepsilon = \left[H^\varepsilon (I, C_0, C_1) \right]^{-1} = B_u^\varepsilon .$$

With a permutation between the inclusions' and the matrix's material characteristics, the inverse M-T model may be easily extracted from the genuine RVE in the third scenario. In this case, the volume proportion of inclusions is so large that they almost completely form a continuous matrix phase. Additionally, it was shown that the M-T and inverse M-T estimates match the Hashin-Shtrikman (H-S) constraints. M-T corresponds to the lower H-S constraint, whereas inverse M-T provides the higher H-S bound, assuming that the inclusions are stiffer than the matrix. Doghri [23] proposed an interpolative D-I model that is described by the following strain concentration tensor connecting the mean strain over the inclusions to its counterpart over the matrix. This model is based on the conclusions of M-T and inverse M-T discussed above.

$$B^\varepsilon = \left[\left(1 - \xi(v_1) \right) \left(B_l^\varepsilon \right)^{-1} + \xi(v_1) \left(B_u^\varepsilon \right)^{-1} \right]^{-1} \tag{2}$$

The $\xi(v_1)$ represents the smooth interpolation function chosen to be simply quadratic.

$$\xi(v_1) = \frac{1}{2} v_1 (1 + v_1) \tag{3}$$

The composite material has designed by using mean field homogenization technique with the help of Mori-Tanaka algorithms and the following properties are found.
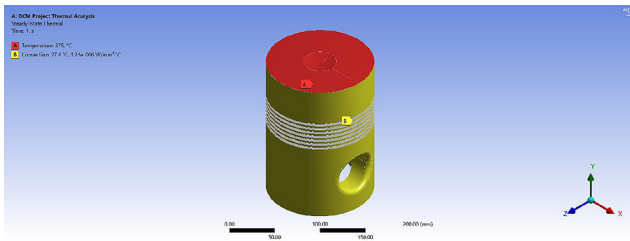
3 Finite element analysis

Thermal and static structural evaluations were carried out separately. Whereas the static structural analysis identified the distribution of deformation and stress, the thermal analysis assessed the distribution of heat and conductivity. The finite element analysis was conducted using ANSYS 18.0 software package [24]. The analysis involves Newton-Raphson method of solver. Elements were of the SOLID186 family, each having a size of 2 mm. Fine grade meshing was applied with a convergence criterion of 10^{-5}. The CAD model file was introduced to ANSYS workbench package. Later, the geometry and topology were cleaned in ANSYS SpaceClaim. Following that, material properties and other conditions were associated with it prior to the analysis as a part of the pre-processing phase. Post analysis, the results were validated with alteration of element types and sizes. However, the mentioned type and size was found to be reliable.

Based on homogenization models and experimental data, the material attributes were assigned. The Nomenclature provided the Young's modulus, Poisson's ratio, and thermal conductivity of 4032 aluminum composites reinforced with graphene and TiO_2. For the thermal analysis (Fig. 2 (a)), the initial temperature was kept as 27.4 °C, based on data of average Indian climatic conditions [4]. The convection coefficient was kept as 1.2410^{-6} W/mm^2 °C. In addition, a temperature of 375 °C was imposed on the piston head. In static structural analysis (Fig. 2 (b)), a 5 MPa pressure was applied on the piston head along with a fixed support in the piston boss.

4 Results and discussion

As shown in Table 1, the density of the graphene-reinforced composites decreased as the weight % of graphene rose, according to the data. Given that graphene is less dense than aluminum, this tendency was anticipated. The composite with 2.5% graphene weight showed the greatest density loss, which was almost 10.5 kg/m^3.
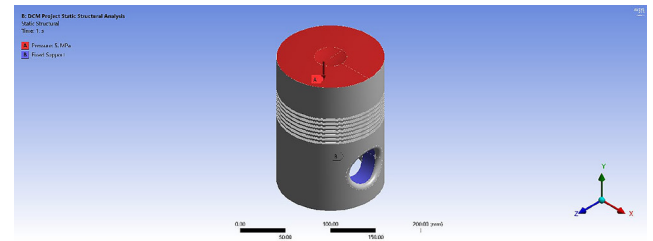
(a)　　　　　　　　　　　　　　　　(b)

Fig. 2 Boundary condition for (a) thermal analysis and (b) static structural analysis

The largest density difference between the composite with 0.5% graphene and the base material without reinforcement was only 2.1 kg/m³, making the density variances between each composite material very minimal. As the weight % of TiO_2 rose, the results for the TiO_2-reinforced composites, on the other hand, revealed an increase in density. This pattern was probably brought about by TiO_2's increased density when compared to aluminum. The composite with 2.5% weight of TiO_2 showed the greatest density gain, which was around 32.8 kg/m³. Similar to the graphene-reinforced composites, the densities of each composite material varied very slightly, with the composite with 2.5% TiO_2 and the base material with no reinforcement differing by a maximum of 32.8 kg/m³.

As the percentage of graphene weight grew, Young's modulus progressively increased as well. In particular, the Young's modulus increased by 3.68% overall as the graphene content increased from 0.5% to 2.5%, as measured in relation to its initial value at 0.5%. Young's modulus increased gradually at each step. On the other hand, TiO_2 content rose from 0.5% to 2.5%, the Young's modulus showed a total increase of 2.20%, calculated relative to its initial value at 0.5%, and the trend held true for intermediate values.

The overall deformation rapidly reduced as the weight percentage of graphene grew, with a maximum drop of around 0.0014 mm being noted in the composite material with 2.5% weight of graphene. This decline can be due to graphene's greater rigidity than aluminum, which resulted in less deformation under a given stress. Similarly, the overall deformation was reduced when TiO_2 was added to the aluminum basis material. The overall deformation reduced progressively as the weight percentage of TiO_2 increased, reaching a maximum increase of around 0.0009 mm in the composite material with 2.5% weight of TiO_2.

The Poisson's ratio rapidly fell as the weight percentage of graphene grew, reaching a maximum decrease of around 0.00238 in the composite material with 2.5% weight of graphene. Due to graphene's greater rigidity than aluminum, which resulted in a lower lateral strain for a given axial strain, this reduction may be credited. Similarly, the Poisson's ratio slightly decreased when TiO_2 was added to the aluminum base material. The Poisson's ratio progressively declined as the weight percentage of TiO_2 increased, reaching a maximum decrease of around 0.00152 in the composite material with 2.5% weight of TiO_2.

The inherent characteristics of the reinforcing materials account for the observed density fluctuations. Because graphene is a lightweight nanomaterial, its density is much lower than that of aluminum, which lowers the overall composite density. Applications with a high strength-to-weight ratio, such internal combustion engine pistons, benefit from this decrease. On the other hand, TiO_2, a ceramic substance that has a density significantly higher than aluminum, adds to the total density of the composite (Fig. 3). This implies that TiO_2 reinforcement may result in heavier components, whereas graphene reinforcement can improve mechanical properties without appreciably increasing weight. The remarkable intrinsic stiffness and robust interfacial bonding of graphene reinforcement with the aluminum matrix, which improves load transfer, are responsible for the rise in Young's modulus (Fig. 4). Because of its high aspect ratio and two-dimensional structure, graphene reduces matrix deformation under applied stress by forming an efficient reinforcing network. On the other hand, TiO_2 has a comparatively lower reinforcing efficiency because of its particle-based morphology and ceramic nature, which may result in stress concentration areas, even though it also improves stiffness. This explains why, in comparison to graphene, the modulus rise with TiO_2 is smaller. Likewise, the decrease in total deformation (Fig. 5) exhibits the similar pattern since graphene's strong stiffness inhibits the spread of strain, while TiO_2 offers some reinforcement but does not limit deformation as much.
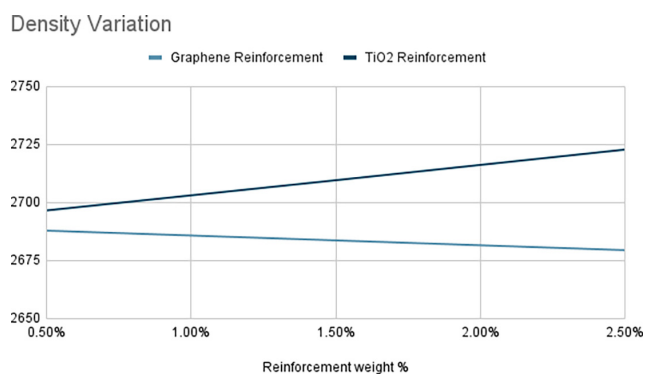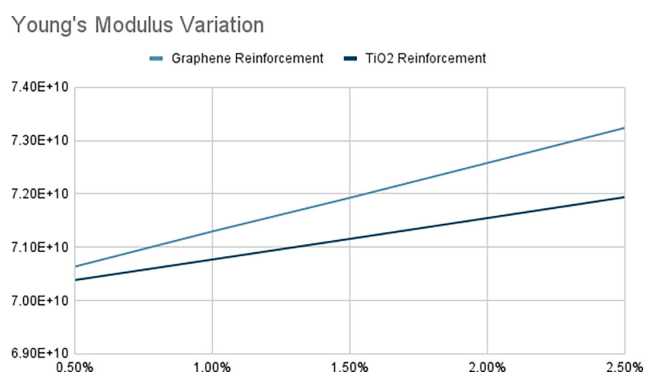

Fig. 3 Density variation plot

Fig. 4 Young's modulus variation plot
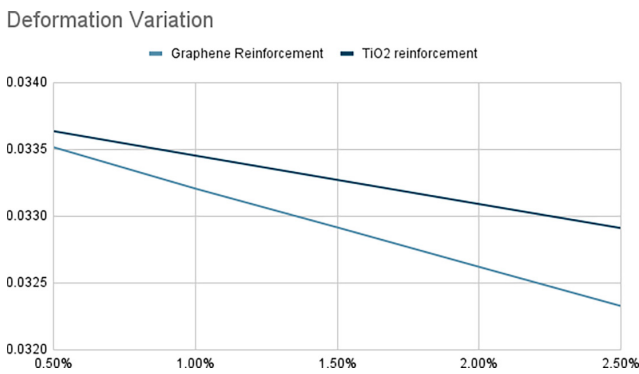
Deformation Variation

Fig. 5 Deformation variation plot

According to temperature trends, TiO_2 may not have as much of an effect on the temperature distribution inside the piston as graphene does when used as a reinforcing material in aluminum composites. Graphene may have a greater impact on the thermal properties of the composite material than TiO_2, even though the differences in temperature increments and decrements between each weight% are relatively small. This is because the overall trend of increasing temperature with graphene and decreasing temperature with TiO_2 is consistent.

The thermal conductance of the graphene-reinforced composite (Fig. 6) increased steadily from 157.13 W/m K to 165.85 W/m K as the weight % of graphene increased. The thermal conductivity of the TiO_2-reinforced composite, on the other hand, decreased as the weight % of TiO_2 increased, with values ranging from 153.89 W/m K to 149.52 W/m K. At the maximum graphene loading, the thermal conductivity of the 4032 aluminum base material and the composite reinforced with graphene differed by 10.85 W/m K, whereas the difference between the thermal conductivity of the 4032 aluminum base material and the composite reinforced with TiO_2 differed by 5.48 W/m K.

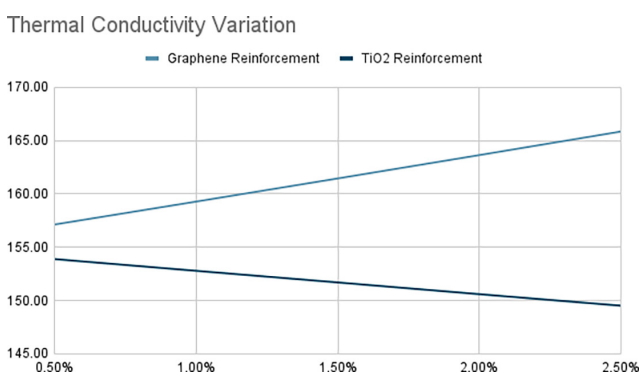When compared to the base alloy, the graphene-reinforced composite showed a 6.99% increase in thermal conductivity (from 155 to 165.85 W/m K) at 2.5 weight percent reinforcement, greatly improving heat dissipation. For piston applications, this enhancement is essential because effective thermal management lowers the risk of overheating, lessens thermal stress, and increases component lifespan. The thermal conductivity of TiO_2-reinforced composites, on the other hand, decreased by 3.54% (to 149.52 W/m K), most likely as a result of the material's higher interfacial resistance and intrinsically lower thermal conductivity. For lightweight, high-heat-flux applications, such as automobile pistons, where quick heat transfer is crucial for longevity and operational efficiency, graphene's better thermal performance and density reduction (0.39% lower) make it the ideal reinforcement.

The statistics shown above allow for the following interpretations along with their:

1. Density: The TiO_2-reinforced composite's higher density as TiO_2 weight percentage increased leads one to believe that the piston created from this material may weigh more than one manufactured from the base material without reinforcement or from the composite reinforced with graphene. The engine's overall performance might be impacted by this weight gain.

2. Poisson's ratio: The TiO_2-reinforced composite's higher Poisson's ratio may indicate that the material is more likely to distort laterally when crushed axially. The piston's durability and stability could be impacted by this.

3. Overall deformation: Since the graphene-reinforced composite has less overall deformation than the base material without reinforcement, it is possible that these materials are stiffer and more resistant to deformation under stress. The piston's performance and durability may benefit from this.

4. Thermal conductivity: The graphene-reinforced composite has a higher thermal conductivity than the TiO_2-reinforced composite or the base material without reinforcement, which implies that it may disperse heat more effectively. This may be crucial for the piston's cooling and the engine's overall performance.

5 Conclusion

This study focused on the impact of graphene and TiO_2 reinforcement on the mechanical and thermal characteristics of the 4032 aluminium alloy for piston applications. The findings demonstrated that, whereas TiO_2 reinforcement enhanced density, graphene's weight % dropped with density of the composites. With graphene reinforcement,

Thermal Conductivity Variation

Fig. 6 Thermal conductivity variation plot

the Poisson's ratio and total deformation went down, but with TiO$_2$ reinforcement, they went up. While it dropped in the TiO$_2$-reinforced composite, the heat conductivity of the graphene-reinforced composite rose. Comparing the two composites, the one based on graphene had a better heat conductivity and a lower density and total deformation. In addition, it has a greater elastic modulus and tensile strength, two characteristics that are essential for a piston to survive high pressure and temperature. However, compared to the TiO$_2$-based composite, the graphene-based composite has a little lower Poisson's ratio. Overall, the advantages of the composite reinforced with graphene exceed the disadvantages, making it a preferable choice for use in pistons:

- Graphene reinforcement (2.5 wt.%) increased Young's modulus by 3.68% (from 7.06×10^{10} Pa to 7.32×10^{10} Pa), outperforming TiO$_2$, which showed a 2.20% increase (from 7.04×10^{10} Pa to 7.19×10^{10} Pa), overall.
- Poisson's ratio decreased by 0.00238 for graphene (0.33 to 0.3276) and 0.00152 for TiO$_2$ (0.33 to 0.3285), indicating graphene's superior resistance to lateral deformation.
- Total deformation under stress is reduced by 0.0014 mm for graphene and 0.0009 mm for TiO$_2$, highlighting graphene's enhanced stiffness.

- Graphene reinforcement improved thermal conductivity by 6.99% (from 155 W/m K to 165.85 W/m K), whereas TiO$_2$ reduced it by 3.54% (to 149.52 W/m K), emphasizing graphene's efficacy in heat dissipation.

Nomenclature

TiO$_2$	Titanium dioxide
MMC	Metal-matrix composites
FEA	Finite Element Analysis
PRMMC	Particle Reinforced Metal Matrix Composites
XRD	X-ray diffraction
FT-IR	Fourier Transform - Infrared Spectroscopy
UV	Ultraviolet
SEM	Scanning electron microscopy
RVE	Representative Volume Elements
D-I model	Double Inclusion model
MFH	Mean-field homogenization
M-T model	Mori-Tanaka model
H-S constraints	Hashin-Shtrikman constraints

References

[1] Javidani, M., Larouche, D. "Application of Cast Al–Si Alloys in Internal Combustion Engine Components", International Materials Reviews, 59(3), pp. 132–158, 2014.
https://doi.org/10.1179/1743280413Y.0000000027

[2] Haque, M. M., Sharif, A. "Study on wear properties of aluminium–silicon piston alloy", Journal of Materials Processing Technology, 118(1–3), pp. 69–73, 2001.
https://doi.org/10.1016/S0924-0136(01)00869-X

[3] Dwivedi, D. K. "Adhesive wear behaviour of cast aluminium–silicon alloys: Overiew", Materials & Design, 31(5), pp. 2517–2531, 2010.
https://doi.org/10.1016/j.matdes.2009.11.038

[4] Kerni, L., Raina, A., Haq, M. I. U. "Performance evaluation of aluminium alloys for piston and cylinder applications", Materials Today: Proceedings, 5(9), pp. 18170–18175, 2018.
https://doi.org/10.1016/j.matpr.2018.06.153

[5] Rogante, M., Lebedev, V. T., Nicolaie, F., Rétfalvi, E., Rosta, L. "SANS study of the precipitates microstructural evolution in Al 4032 car engine pistons", Physica B: Condensed Matter, 358(1–4), pp. 224–231, 2005.
https://doi.org/10.1016/j.physb.2005.01.240

[6] Nur Cahyo, F., Soegijono, B. "Effect of Solution Heat Treatment of Aluminum Alloy 4032 on the Structure and Corrosion Resistance in 3,5% and 10,5% NaCl Solution", IOP Conference Series: Materials Science and Engineering, 694, 012043, 2019.
https://doi.org/10.1088/1757-899X/694/1/012043

[7] Magibalan, S., Senthil Kumar, P., Vignesh, P., Prabu, M., Balan, A. V., Shivasankaran, N. "Aluminium Metal Matrix Composites - A review", Transactions on Advancements in Science and Technology, 1(2), pp. 1–6, 2017.

[8] Rao, S. R., Padmanabhan, G. "Fabrication and mechanical properties of aluminium-boron carbide composites", International Journal of Materials and Biomaterials Applications, 2(3), pp. 15–18, 2012.

[9] Ravichandran, M., Naveen Sait, A., Anandakrishnan, V. "Synthesis and forming behavior of aluminium-based hybrid powder metallurgic composites", International Journal of Minerals, Metallurgy, and Materials, 21(2), pp. 181–189, 2014.
https://doi.org/10.1007/s12613-014-0883-z

[10] Balasivanandha Prabu, S., Karunamoorthy, L. "Microstructure-based finite element analysis of failure prediction in particle-reinforced metal-matrix composite", Journal of Materials Processing Technology, 207(1–3), pp. 53–62, 2008.
https://doi.org/10.1016/j.jmatprotec.2007.12.077

[11] Sozhamannan, G. G., Prabu, S. B., Paskaramoorthy, R. "Failures analysis of particle reinforced metal matrix composites by microstructure based models", Materials & Design, 31(8), pp. 3785–3790, 2010.
https://doi.org/10.1016/j.matdes.2010.03.025

[12] Tiwari, S. K., Sahoo, S., Wang, N., Huczko, A. "Graphene research and their outputs: Status and prospect", Journal of Science: Advanced Materials and Devices, 5(1), pp. 10–29, 2020.
https://doi.org/10.1016/j.jsamd.2020.01.006

[13] Tiwari, S. K., Kumar, V., Huczko, A., Oraon, R., Adhikari, A. D., Nayak, G. C. "Magical allotropes of carbon: prospects and applications", Critical Reviews in Solid State and Materials Science, 41(4), pp. 257–317, 2016.
https://doi.org/10.1080/10408436.2015.1127206

[14] Kashinath, L., Kumar, R. S., Hayakawa, Y., Ravi, G. "Synthesis & Structural Study on Graphene Particles", International Journal of Science and Engineering Applications, Special Issue NCRTAM, pp. 8–12, 2013.
https://doi.org/10.7753/IJSEANCRTAM.1003

[15] Dahl, M., Liu, Y., Yin, Y. "Composite Titanium Dioxide Nanomaterials", American Chemical Society, 114(19), pp. 9853–9889, 2014.
https://doi.org/10.1021/cr400634p

[16] Abass, B. A., Hunain, M. B., Khudair, J. M. A. "Effects of Titanium Dioxide Nanoparticles on the Mechanical Strength of Epoxy Hybrid Composite Materials Reinforced with Unidirectional Carbon and Glass Fibers.", IOP Conference Series: Materials Science and Engineering, 1094, 012159, 2021.
https://doi.org/10.1088/1757-899X/1094/1/012159

[17] Maryin, D., Glushchenko, A., Khokhlov, A., Proshkin, E., Mustyakimov, R. "Results of engine tests of an experimental gasoline internal combustion engine", BIO Web of Conferences, 17, 00078, 2020.
https://doi.org/10.1051/bioconf/20201700078

[18] Pierard, O., Friebel, C., Doghri, I. "Mean-field homogenization of multi-phase thermo-elastic composites: a general framework and its validation", Composites Science and Technology, 64(10–11), pp. 1587–1603, 2004.
https://doi.org/10.1016/j.compscitech.2003.11.009

[19] Sharma, A., Rastogi, V., Agrawal, A. K. "Estimation and Experimental Validation of Mean-Field Homogenised Effective Properties of Composite", Experimental Techniques, 45(4), pp. 445–456, 2021.
https://doi.org/10.1007/s40799-020-00411-7

[20] Punera, D., Kant, T. "A critical review of stress and vibration analyses of functionally graded shell structures", Composite Structures, 210, pp. 787–809, 2019.
https://doi.org/10.1016/j.compstruct.2018.11.084

[21] Peng, X., Hu, N., Zheng, H., Fukunaga, H. "Evaluation of mechanical properties of particulate composites with a combined self-consistent and Mori–Tanaka approach", Mechanics of Materials, 41(12), pp. 1288–1297, 2009.
https://doi.org/10.1016/j.mechmat.2009.07.006

[22] Nemat-Nasser, S., Hori, M. "Micromechanics: overall properties of heterogeneous solids", Elsevier Science Publishers, 1993. ISBN 0-444-89881-6

[23] Doghri, I. "Micro-mechanics of materials", In: Mechanics of Deformable Solids: Linear, Nonlinear, Analytical and Computational Aspects, Springer, 2000, pp. 519–544. ISBN 978-3-642-08629-8
https://doi.org/10.1007/978-3-662-04168-0_20

[24] ANSYS, Inc "ANSYS (18.0)", [computer program] Available at: https://www.ansys.com/it-solutions/platform-support/previous-releases [Accessed: 31 December 2024]